1966

Mechanism of Current Conduction through Precipitated Fly-Ash

O J. Tassicker

Z Herceg

K McLean

Mechanism of Current Conduction through Precipitated Fly-Ash

BULLETIN No. 10

WOLLONGONG UNIVERSITY COLLEGE
THE UNIVERSITY OF NEW SOUTH WALES

Mechanism of Current Conduction through Precipitated Fly-Ash

O.J. Tassicker Z. Herceg K. McLean

DIVISION OF ENGINEERING

FEBRUARY, 1966

MECHANISM OF CURRENT CONDUCTION THROUGH

PRECIPITATED FLY-ASH

O.J. TASSICKER Z. HERCEG K.J. McLEAN

Department of Electrical Engineering
Wollongong University College,
The University of New South Wales.

February 1966.

CONTENTS PAGE

SYNOPSIS

An experimental determination and a new analytical approach to the process of current conduction in a high resistivity powder is described. Extensive experimental determinations of the relationship between current density, potential gradient, conductivity and absolute temperature show that the powder apparently behaves as an intrinsic semi-conductor. At elevated temperatures, the classical relationship :-

$$\sigma = K \epsilon^{\frac{-E_f}{kT}} \text{ holds.}$$

A new theory of the conduction mechanism is developed. It shows that the classical conductivity relationship is more apparent than real. Current transfer is considered to take place both within solid particles by conduction and between them by a Schottky-type field-enhanced thermionic emission. The mean geometry of the particles, viz, size and separation are defined. In this way, current density, voltage-gradient relationships are deduced in terms of absolute temperature, particle geometry and conductivity. Such analytical results follow the experimental results closely. By curve fitting, the experimental data leads to important microscopic and macroscopic information about the dust, its size and Fermi level.

The use of this new analytical approach may provide important information, such as the effect of moisture or adsorbed gases, on the conductivity of semi-conducting particles.

The experiments have all been performed on a planar electrode system, using dry particles at elevated temperatures.

The experiments were all performed on fly-ash taken from the precipitator hoppers of N.S.W. power stations. A prime objective is to obtain a better understanding of the difficulties in precipitator operation accruing from the very high resistivity of the dusts encountered.

SYMBOLS

R	resistance between electrodes, ohm
$\sigma = \sigma_{av}$	conductivity of bulk material $ohm^{-1}\ m^{-1}$
σ	conductivity of a single particle, $ohm^{-1}\ m^{-1}$
ρ	resistivity of bulk material, $ohm^{+1}\ m^{+1}$
D	distance between electrodes, m
A	area of receiving electrode, m^{+2}
k	Boltzmann's constant (1.38×10^{-23}) joule $^{o}K^{-1}$
T	absolute temperature, ^{o}K
V	potential difference, Volt
$F = F_{av}$	potential gradient between electrodes, $V^{+1}\ m^{-1}$
F_a	potential gradient in gap between particles $V^{+1}\ m^{-1}$
q	electronic charge (1.602×10^{-19}), coulomb
m	electronic mass (9.107×10^{-31}), kilogram
J	nett current density, $A^{+1}\ m^{-2}$
J_o	current density between particles in absence of external field $A^{+1}\ m^{-2}$
x	distances normal to surface and in the direction of the applied field, m.
v_x	electron velocities in the x direction, $m^{+1}\ sec^{-1}$

Symbols, (continued).

E_f	Fermi energy level, between conduction and valence bands, eV
E_o	width of forbidden zone, eV
W	energy difference between bottom of conduction band and vacuum level, eV
2a	average separation between particles, m^{+1}
d	average normalised particle size between successive gaps, m^{+1}
A_a	gap area between particles, m^{+2}
A_d	average cross-sectional area of solid particle, m^{+2}
eV	electron volts
C, K	constants.

1. INTRODUCTION

One of the fundamental processes taking place in electrostatic precipitators is the conduction of electric charge through the layer of particles precipitated on the collecting plate. As the particles enter the electrostatic precipitator they are charged negatively by the corona current flowing between the electrodes. The strong electric field between these electrodes exerts a force on the particles and deposits them on the collecting plate forming a thin layer of dust. As further charged particles are collected they lose their charge by discharging through the existing layer to the plate.

The mechanism of this current conduction through the layers of precipitated particles is important to the operation of electrostatic precipitators. The corona current causes a high voltage gradient to develop across the layer of particles, the value being dependent on the total current and the resistivity of the particles. For particles of high resistivity, the magnitude is such that the effective gradient in the air gap between the dust layer and the emitting electrode is reduced and

the efficiency is adversely affected. A more serious phenomenon is also established. With high resistivity particles, 2×10^{10} ohm cm and above, blue point discharges take place in the dust called "back corona". This has the effect of reducing the spark-over voltage of the precipitator[1,2], and hence its efficiency. This phenomenon is not observed in dust of low resistivity.

A considerable amount of experimental work has been done in an effort to explain the mechanism of this conduction. It has been generally assumed[3,4], that there are two processes taking place :

(a) Volume conduction

(b) Surface conduction.

Volume conduction takes place through the main body of the material and the magnitude of the current depends on the composition of the particles and the temperature. It has been shown experimentally[4] that the layer has the same conducting characteristics as other dielectrics. The conductivity increases with rising temperature and follows the exponential law :

$$\sigma = \frac{1}{\rho} = K \epsilon^{-\frac{E_f}{kT}} \qquad \ldots\ldots\ldots\ldots\ldots (1)$$

Surface conduction takes place over the surface of the particles when they have been conditioned with moisture or special chemicals. A thin film is formed on the surface due to adsorption and conduction takes place through it. The actual mechanism of conduction is not very well understood but it appears to be electrolytic or ionic in character with the proton jump mechanism [6] being the predominant method of charge transfer. Much experimental work[3,6], has been carried out to determine the influence that moisture and conditioning agents in the gas stream have on the surface conductivity of the particles.

It is generally assumed that the surface conductivity predominates in most precipitators and that volume conductivity only is significant at more elevated temperatures.

An associated problem is the measurement of the particle resistivity. This may be done by using either the parallel plane or the point plane system[4]. Lakey and Bostock have found that both methods give good agreement within the limits of accuracy of the apparatus. Sproull and Nakada[7] have described a laboratory apparatus that is used to measure the resistivity

of dust particles conditioned by gases. Laboratory measurements are suitable for making comparison of dusts and for determining the effect of conditioning agents but they cannot accurately reproduce the condition of the particles in the precipitator. Cohen and Dickinson[8] have described an apparatus suitable for measuring the resistivity of fly-ash "in situ.". The fly-ash is collected by a cyclone and its resistivity is measured by means of a small concentric cylinder cell.

2. SCOPE

Although a considerable amount of research has been done there are still many unsolved problems with regard to charge conduction through layers of high resistivity particles, especially with reference to the fly-ash in New South Wales. An extensive programme of research is being planned by the Electrical Engineering Department at Wollongong University College of The University of New South Wales to investigate this and other problems associated with electrostatic precipitation.

A suitable starting point seemed to be the investigation of the volume conductivity of fly-ash. This Bulletin is, therefore,

restricted to this aspect of the project and records the progress already made. It also extends the work given in the preliminary report[9] by the authors.

3. MEASUREMENTS

3.1 APPARATUS

The apparatus used to measure the resistivity of the fly-ash is shown in Fig.1. It consists principally of two parallel plates with a guard ring around the bottom plate. Any leakage or end effect current flows to this ring and is so connected in the circuit to bypass the measuring instrument. The top bearing is made of P.T.F.E.* and serves the double purpose of holding the top electrode in position and insulating it from the rest of the apparatus. This electrode can be moved freely in the vertical axis and can be adjusted in the horizontal axis by means of three vertical supports. The fly-ash to be measured is held in position by means of a P.T.F.E. cylindrical container.

Temperature measurements were made by a chromel alumel thermocouple placed between the guard ring and the P.T.F.E. cylindrical container.

---

* Polytetrafluorethylene, commonly known as Teflon.

3.2 CIRCUIT

The circuit connections are shown in Fig.2.

The top electrode of the apparatus is energized negatively by a high voltage d.c. supply. The current flowing through the bottom plate is measured by a micro-ammeter. This instrument is a Philips GM 6020 Microvoltmeter connected to measure current. A Philips voltmeter type GM 6009 in conjunction with the high tension probe type GM 4579B is used to measure the voltage. The connection of the bottom electrode to the micro-ammeter is via P.T.F.E. insulated coaxial screened cable, the guard ring current being carried by the screening. The instruments, screening, guard ring and oven were all carefully earthed and considerable care was necessary to eliminate the effects of external fields.

3.3 PROCEDURE

The depth of the dust between the electrodes was measured by means of a dial gauge attached to a stand. This was mounted on the top frame as shown in Fig.1., the height of the central shaft being measured without any fly-ash and with the top electrode

resting on the bottom electrode. The fly-ash was then very carefully placed in the apparatus so as to ensure even compactness, the top electrode being carefully lowered so as to make contact over the whole surface of the fly-ash. The height of the shaft was again measured and the difference in readings gave the depth. This measuring procedure was repeated at the end of the test while all equipment was hot. The average fly-ash depth was then calculated.

Since all measurements were performed at elevated temperatures the apparatus was placed in an oven. The oven temperature was initially adjusted to its maximum temperature of 550°F and left at this value for over ten hours. This ensured uniform temperature and total dryness of the dust. To obtain consistant results it was found necessary to apply maximum voltage across the fly-ash for a short time. This allowed the particles to settle, consistent results then being obtained. The maximum voltage applied was well below the ionization level. A series of voltage and current readings were taken. For each voltage change it was necessary to allow the current to settle before

taking the reading. To change the temperature of the fly-ash the oven setting was lowered and the temperature allowed to settle to its new value before making further measurements. Steady state conditions were indicated by the thermo-couple.

The resistivity ρ of the dust was calculated from the relationship

$$\rho = \frac{1}{\sigma} = \frac{RA}{\ell} \qquad (2)$$

3.4 ACCURACY

The main errors introduced by the measuring apparatus are listed in the following table

QUANTITY MEASURED	ERROR
VOLTAGE	± 3%
CURRENT	± 3%
TEMPERATURE	± 3%
LAYER DEPTH	± 1%

The error introduced due to uneven compactness is uncertain. Considerable care was taken to ensure as even and consistent compaction as possible but no certainty can be obtained until a better method of compacting the fly-ash is devised.

The results at one temperature but different thicknesses do show good agreement, most points being within ± 10% of the mean value.

4. RESULTS

4.1 Current-density/Voltage-gradient Relationships

Fig. 3 shows the voltage gradient/current density characteristics of the fly-ash. Measurements were made with four different depths of fly-ash in the measuring apparatus and at four different temperatures for each depth of fly-ash. It was found impossible to adjust the temperature to the same value for the different depths so the necessary correction has been made before plotting. These curves show that :

(a) voltage-current relationship is not linear and that

(b) the depth of fly-ash in the measuring apparatus does not

affect the result. The small scatter in the results of Fig. 3 is probably due to uneven compactness.

These results can be plotted in two other forms which are of considerable value in interpreting the results. Fig. 4 shows the voltage-gradient/current-density characteristics at one temperature plotted on linear co-ordinates. Fig. 5 shows a plot of conductivity/ $\frac{1,000}{T}$ for one depth of fly-ash.

4.2 EFFECT OF COMPACTION

A preliminary investigation was also made into the effect of compaction. The results are shown plotted in Fig. 6. Curve A shows the voltage-gradient/current density relationship for moderate compaction. Curves B and C show the relationships with greater amounts of compaction. The bulk density figures are relative values only and are based on the weight of fly-ash per unit volume. The bulk density of curve A is taken as the reference and is given a value of 1.0.

5. MECHANISM OF CURRENT CONDUCTION

It is assumed that two basic processes determine the steady-state current flow,

(a) electron emission between particles, and

(b) drift current within particles.

Considering that the distance between particles,* where the current transfer occurs, is of the order of 10^{-8}m, the presence of air in gaps should not affect the emission current, because the distance of 10^{-8}m is much smaller than the mean free path of electrons in air under given conditions. Space charge within individual particles can be neglected in comparatively thick layers, even if the diffusion length is not much larger than the particle size.

5.1 ANALYSIS OF CURRENT CONDUCTION

The average energy level diagram without the applied field is shown in Fig. 7.

---

* The Stokes-equivalent mean particle size is about 5 micron.

Assuming the theoretical $T^{-3/2}$ law for a lattice-scattering mobility, and applying the Fermi-Dirac statistical distribution the following well-known expression (after equation 1) is obtained for an intrinsic semiconductor[10].

$$\sigma = K \epsilon^{\frac{-q E_f}{kT}} = K \epsilon^{\frac{-q E_o}{2kT}} \quad \ldots\ldots(3)$$

Only these electrons in the conduction band having the kinetic energy $\frac{1}{2} m v_x^2 \geq W - \phi_{max.}$ can be exchanged between particles. The corresponding current of density

$$J_o = J_{12} = -J_{21} = C T^2 \epsilon^{\frac{-q(E_f + W - \phi_{max.})}{k T}} \quad \ldots(4)$$

flows across the barrier in both directions. The total current density without the applied field is zero

$$J = J_{12} - J_{21} = 0 \quad \ldots\ldots(5)$$

When the average field $F_{av} = \frac{V}{D}$ (V, applied voltage; D, distance between electrodes) is applied, the energy level diagram is changed as shown in Fig.8.

Field in the gap, F_a, reduces the potential barrier approximately to

$$W - \phi_{a\ max.} \simeq W - \phi_{max.} - q\, a\, F_a \quad \ldots\ldots (6)$$

The position of the maximum is approximately half-way between the particles, i.e. $X_{max.} \ll 2a$.

Distances 2a and d are, respectively, the average gap width and the average length of the current path in solid between two gaps.

In this model, the same current density is assumed in the gap and in the solid. Consequently, the distance d is a "normalised" real distance between two gaps, d_d.

$$d = d_d \frac{A_a}{A_d} ,$$

where A_a is the gap area, and A_d is the average cross-section area of the solid.

Correlation between experimental results and relationships derived from this model is possible only for a particular density and geometry of particles, because the electrode area

determines the measured current density and the areas A_a and A_d remain unknown.

With the direction of F_{av} as indicated in Fig.8, the current J_{12} is enhanced and the current J_{21} suppressed, because the effective work function for the transition $1 \rightarrow 2$ becomes

$$\phi_{12} = E_f + W - \phi_{max.} - q\,a\,F_a$$

and for the transition $2 \rightarrow 1$ . . . . (7)

$$\phi_{21} = E_f + W - \phi_{max.} + q\,a\,F_a$$

Hence, the total current density with the field F_{av} applied is

$$J = J_{12} - J_{21} = J_o \left(\epsilon^{\frac{q\,a\,F_a}{kT}} - \epsilon^{\frac{-\,q\,a\,F_a}{kT}} \right) = 2\,J_o \sinh \frac{q\,a\,F_a}{kT}$$

. . . . (8)

Field in the gap, F_a, can be determined from the voltage drop over the distance $(2a + d)$,

$$F_{av}\,(2a + d) = \frac{J}{\sigma'}\,d + 2a.F_a \qquad \ldots\ldots (9)$$

$$F_a = F_{av}\,\frac{2a + d}{2a} - \frac{J}{\sigma'} \cdot \frac{d}{2a} \cdot$$

The implicit form for the current density, J, as a function of the applied field, F_{av}, is obtained by substituting F_a,

$$J = 2 J_o \sinh \left[\frac{q}{kT} \left(F_{av} \frac{2a + d}{2} - \frac{J}{\sigma'} \cdot \frac{d}{2} \right) \right] \quad . \quad . \quad . (10)$$

$$J \simeq 2J_o \sinh \left[\frac{qd}{2kT} \left(F_{av} - \frac{J}{\sigma'} \right) \right] \quad . \quad . \quad . (11)$$

This function, shown in Fig. 9, has the asymptote with the slope

$$\left(\frac{\partial J}{\partial F_{av}} \right)_{J \to \infty} = \sigma' \left(1 + \frac{2a}{d} \right) \simeq \sigma' \quad . \quad . \quad . \quad . \quad (12)$$

Obviously, the apparent conductivity $\sigma = \sigma_{av} = \frac{J}{F_{av}}$ is a function of the applied field and is always smaller than the conductivity σ' (which represents the conductivity of the solid between electrodes), but it is a function of density and geometry of particles.

For large current densities also the potential distribution becomes uniform, i.e.

$$\frac{J}{\sigma'} \to F_{av} \, , \quad F_a \to F_{av} ,$$

and the potential barriers between particles approach zero,

This means that at low stresses the gap barrier is the main factor determining the current, and at high stresses current is ultimately limited only by the conductivity of solid.

5.2 FITTING RESULTS

The numerical analysis of experimental results for the particular dust yielded the following quantitative relationships.

$$J = 2\, J_o \sinh \left[\frac{3.65.10^{-3}}{T} \left(F_{av} - \frac{J}{\sigma'} \right) \right]$$

$$J_o = 7.10^{-3}\, T^2\, \epsilon^{\frac{-9900}{T}} \qquad \ldots\ldots (13)$$

$$\sigma' = 2.35.10^{-2}\, \epsilon^{\frac{-9690}{T}}$$

The evaluated equation for the current density, $J = f(F_{av})$ is plotted along with experimental results in Fig.3.

Relating these fitting equations back to the theoretical emission model, the Fermi level is found to be

$$E_f = 0.835 \text{ eV},$$

and the gap barrier

$$W = \phi_{max.} = 0.018 \text{ eV}.$$

The "normalised" average current path in solid between two gaps is

$$d = 5.26.10^{-7} \text{ m},$$

and the gap between particles, approximately,

$$2a \simeq 2\left[\frac{W - \phi_{max.}}{F_{av}}\right]_{J \to \infty} < 2.10^{-8} \text{ m}.$$

5.3 DISCUSSION ON THE METHODOLOGY

The initial assumption, that fly-ash can be regarded as an intrinsic semi-conductor, Equation (1), is justified only at elevated temperatures. Validity of the analysis is restricted to the linear part of the curve $\sigma_{av} = f(\frac{1}{T})$, shown in Fig. 5.

Current transfer mechanism between particles is not necessarily the field enhanced thermionic emission only. It is possible that a certain proportion of current is carried by electrons tunnelling through the thin potential barrier. This particularly applies under high stresses. Then the field in a gap can attain the value of $10^8 \frac{V}{m}$ or more. The significance of numerous contact barriers is reasonably confirmed by current

density - average field characteristics being independant of sample thickness. That implies also macroscopically uniform potential distribution.

The fact that, under all conditions, the current is increased with compactness of dust, can be accounted for by the increased number of parallel, minimum energy current paths, i.e. effectively larger conducting area. This explanation is supported by measurements on samples of different compaction, with results plotted in Fig. 6. Curves in Fig. 6 differ, at least in the first approximation, only by a constant factor.

In the expression for current density, J, the compaction of dust affects directly the coefficient, J_o, and conductivity, σ', but not the average distance between two gaps, d (which is presumably the function of particle shape and size distribution). Since the change of J_o is predominant, the increased density of dust corresponds in the first instance to a larger coefficient, J_o'. The relationship between the density and J_o has not been studied. However, it can be accepted that different coefficients,

J_o, obtained from measurements on samples of the same dust, indicate varying density of samples. Hence, the conspicuous deviation of the 0.15" sample in Fig.3 can be attributed to non-uniform density. With less pronounced deviations it is difficult to distinquish between measuring errors, temperature, stray and compactness effects.

Obviously, it is not possible to achieve precision in measurements without adequate techniques for preparing samples of uniform and reproducible density.

6. CONCLUSIONS

From extensive current-voltage, current temperature and density-effect measurements, important information may be deduced concerning both the microscopic and macroscopic nature of a conducting powder. For instance the conductivity of the solid particles (σ') and their Fermi-Level (E_f) may be isolated from parameters characterising dust structure viz: particle size, density, contact barrier and the distance between gaps.

The number of parameters which can be evaluated makes this method suitable for comparing different dusts, or correlating with constituents of a complex material like fly-ash. Also, the effects of additives such as conditioning gases, moisture etc. may be more precisely determined.

REFERENCES

1. PENNY and CRAIG, "Sparkover as Influenced by Surface Conditions in D.C. Corona". A.I.E.E. Trans. Pt.1 vol. 79, (1960).

2. PENNY and CRAIG, "Pulsed Discharges Preceding Sparkover at Low Voltage Gradients" A.I.E.E. Trans Pt.1 vol. 80 (1961).

3. H. J. WHITE, "Industrial Electrostatic Precipitators" Addison-Wesley Publishing Co.

4. J. LAKEY and W. BOSTOCK, "Researches into Factors Affecting Electro-precipitation". Trans. I. Chem. E., Vol. 33, (1955).

5. J. D. BERNAL and J. FOWLER, "A Theory of Water and Ionic Solutions" J. Chem. Phys. 1, p 515 (1933).

6. R. O. DANIELS, "A Study of Adsorbed Films Upon the Surface Electrical Conductivity of Powders". Ph.D. Thesis, University of Utah.

References (continued)

7. W. T. SPROULL and Y. NAKADA. "Operation of Cottrell Precipitators" Ind. Eng. Chem. 43, 1250 (1951)

8. L. COHEN, and R. W. DICKINSON. "The Measurement of the Resistivity of Power Station flue dust". J. Sci. Inst. Vol. 40 (1963).

9. O. J. TASSICKER Z. HERCEG and K. J. McLEAN. "The Electrical Resistivity of Precipitator Fly-Ash. Bulletin No. 7. W.U.C. of U.N.S.W. 1965.

10. C. KITTEL. "Introduction to Solid State Physics". Wiley & Sons, 1953, pp. 275 - etc.

APPENDIX.

8. PHYSICAL AND CHEMICAL DATA

8.1. CHEMICAL ANALYSIS (A)

A chemical analysis of the fly-ash is given in the following table :-

COMPOUND	PERCENT CONTENT
Combustible	2.4
SiO_2	71.3
Al_2O_3	21.6
Fe_2O_3	2.8
CaO	0.96
NgO	0.22
S and SO_3	0.22

The above table is of interest because it shows that 93% of the fly-ash is made up of SiO_2 and Al_2O_3.

8.2. X-RAY DIFFRACTION PATTERN (B)

An X-Ray diffraction pattern was taken to determine the mineral combination of the silica and alumina. As yet, no definite conclusions have been arrived at. The fly-ash has a pattern similar to that of silimanite. It is also considered that the basic oxides present in the ash are probably in solution in the alumino-silicate. The conclusion that the ash consists of an alumino-silicate of the silimanite type cannot account for some 50 per cent of the SiO_2. Since the diffraction patterns shows no strong lines this would indicate that some polymorph of this oxide is present. One possible conclusion that may be drawn is that this SiO_2 is present in a non-crystalline form, either as SiO_2 or in some complex molecular form.

References (A) Data supplied by Electricity Commission of New South Wales.

(B) Tests conducted and analysed by Department of Metallurgy, Wollongong University College of The University of New South Wales.

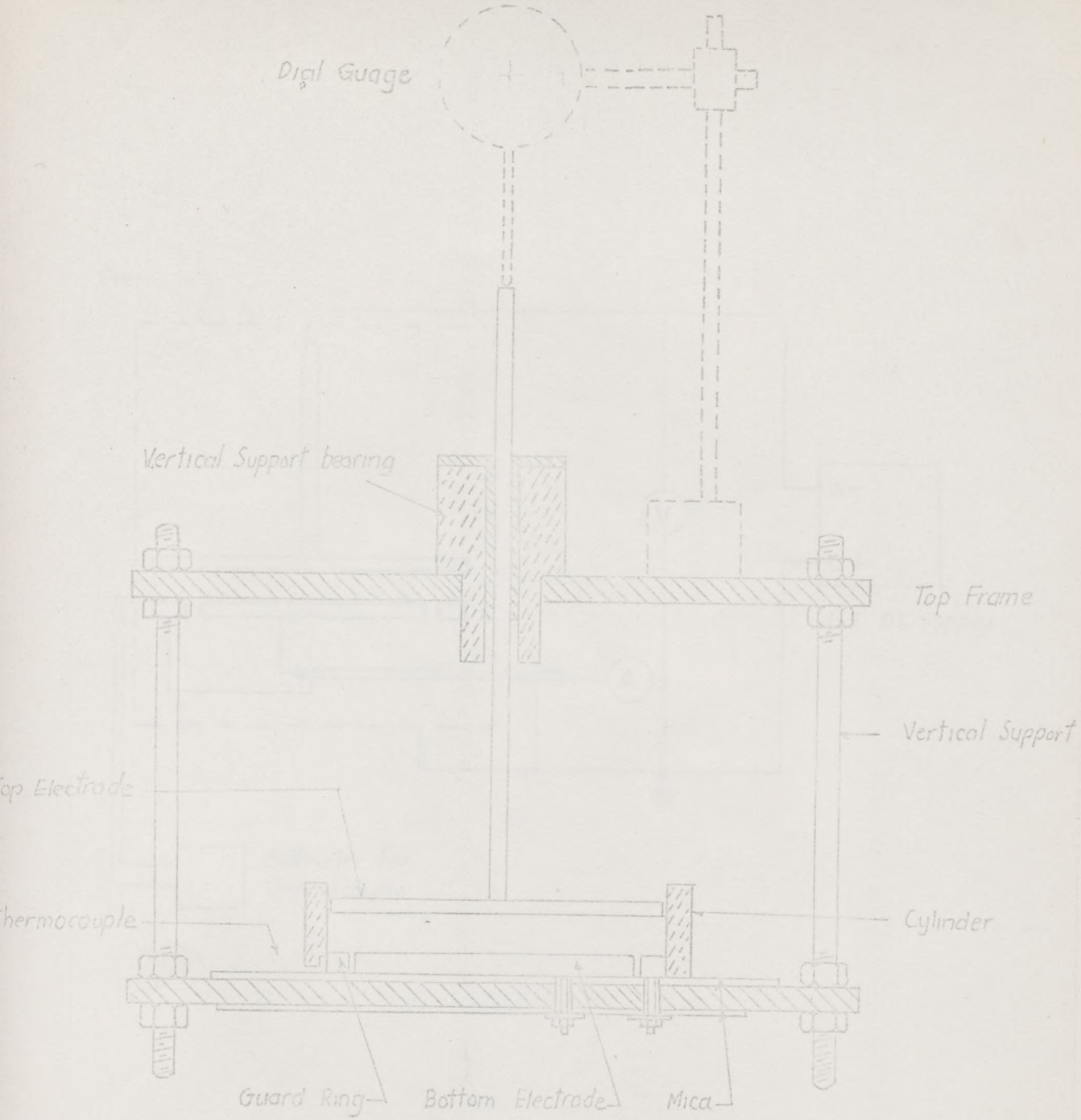

Fig. 1 THE RESISTIVITY MEASURING APPARATUS

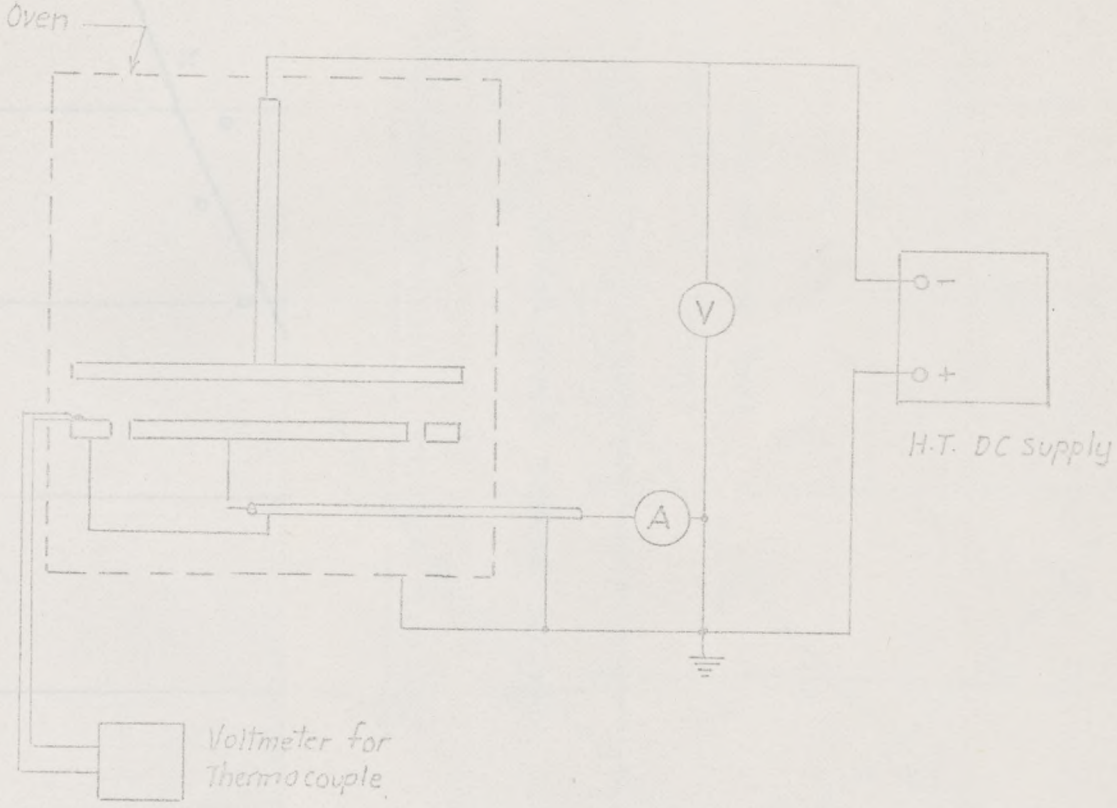

Fig 2. DIAGRAM OF CONNECTIONS

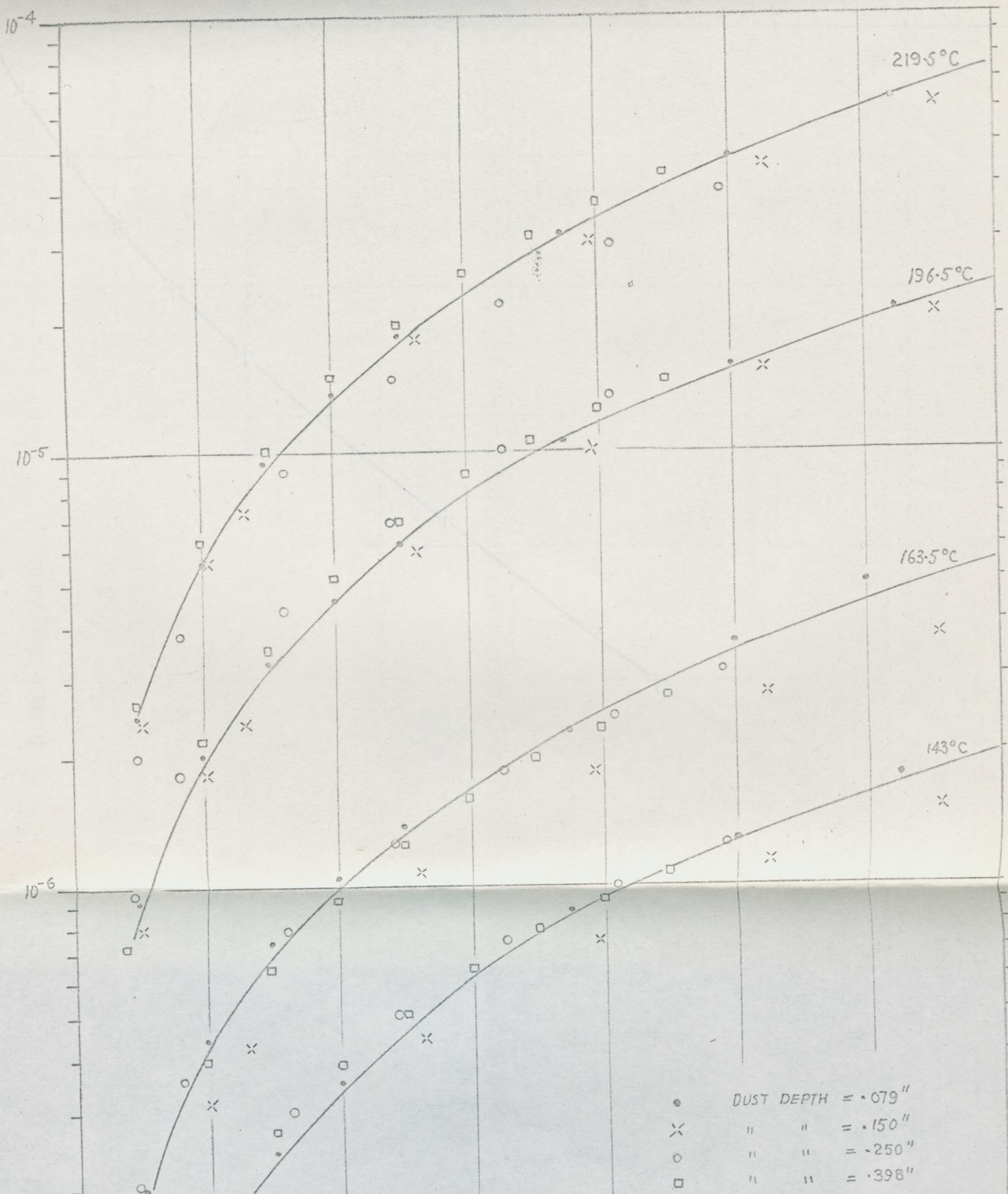
10^{-4}
10^{-5}
10^{-6}
219·5°C
196·5°C
163·5°C
143°C
CURRENT DENSITY (AMPS / METER²)
DUST DEPTH = ·079"
" " = ·150"
" " = ·250"
" " = ·398"

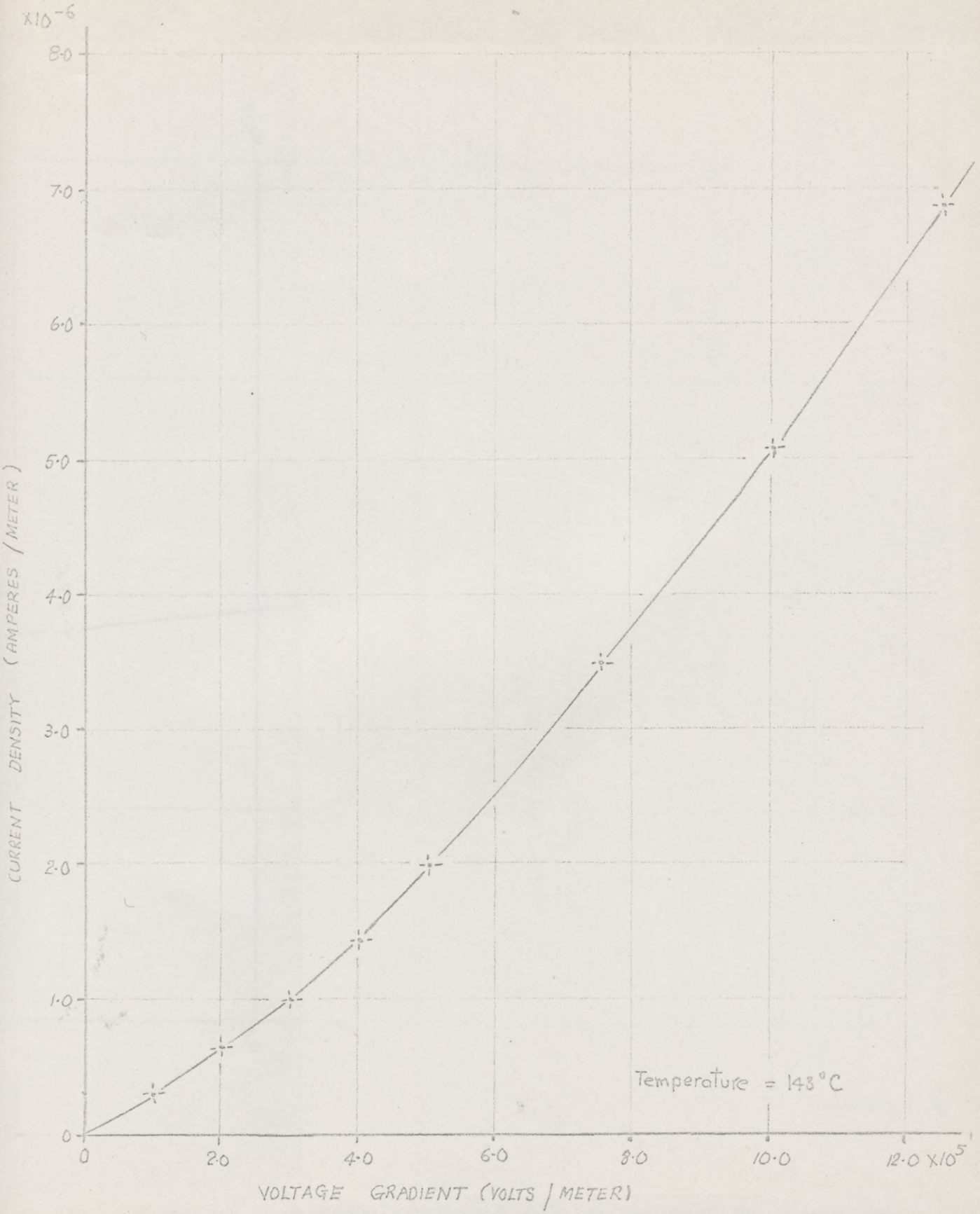

Fig. 4 A TYPICAL CURRENT DENSITY / VOLTAGE GRADIENT CURVE

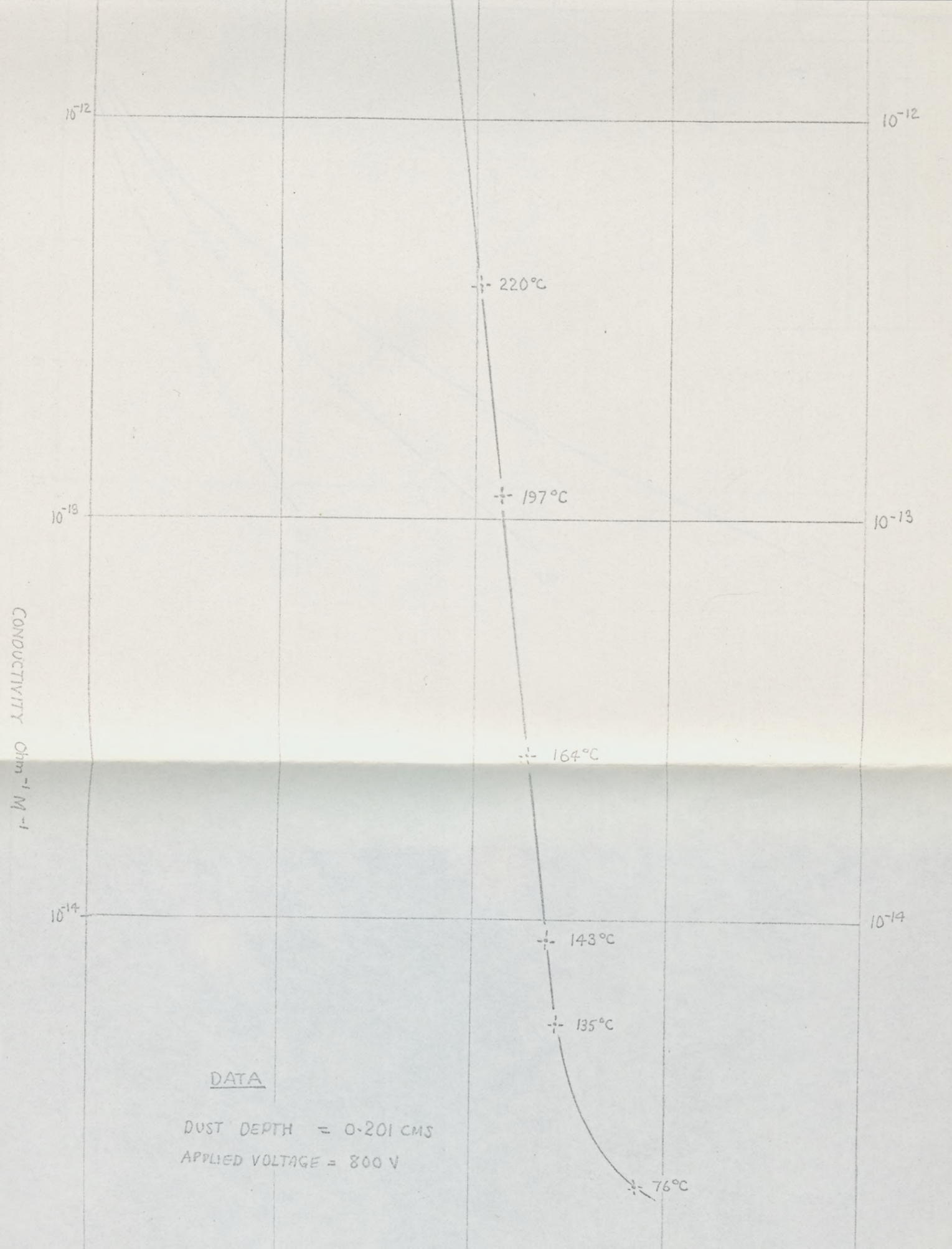
10^{-12}
10^{-13}
10^{-14}
220°C
197°C
164°C
143°C
135°C
76°C
CONDUCTIVITY ohm^{-1} M^{-1}
DATA
DUST DEPTH = 0·201 CMS
APPLIED VOLTAGE = 800 V

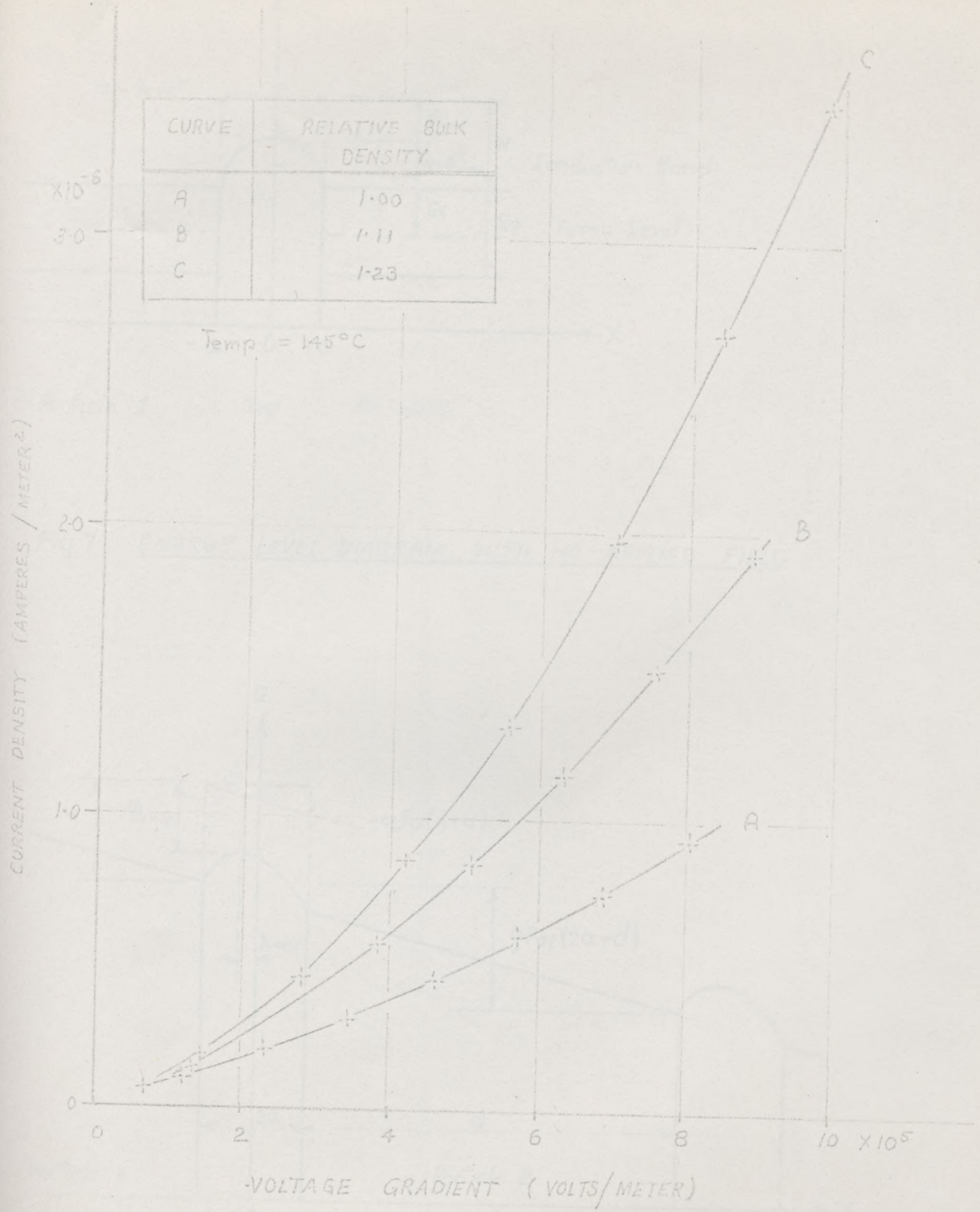

Fig 6 VOLTAGE GRADIENT/CURRENT DENSITY RELATIONSHIPS WITH VARIATION OF BULK DENSITY

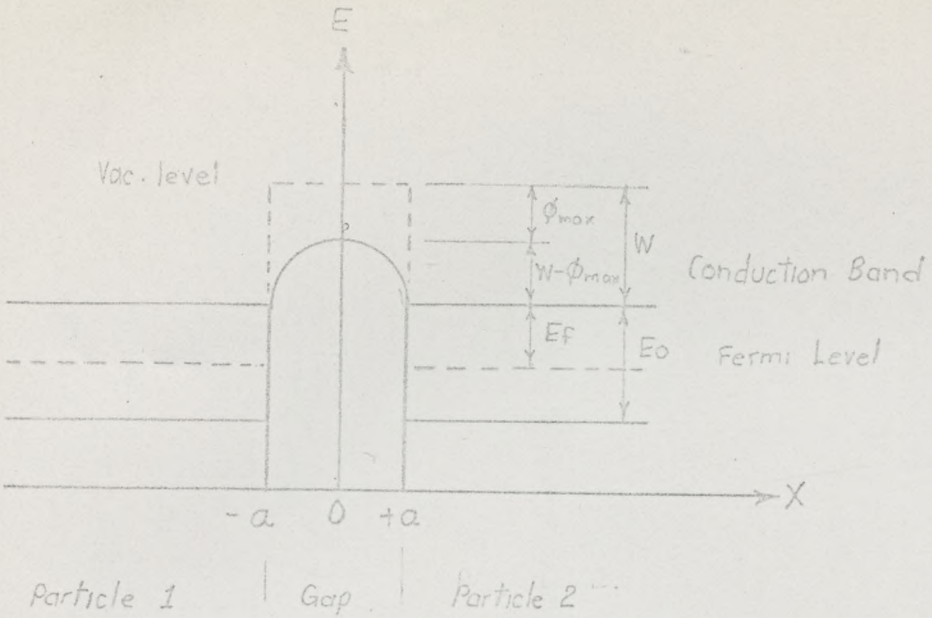

Fig 7 ENERGY LEVEL DIAGRAM WITH NO APPLIED FIELD

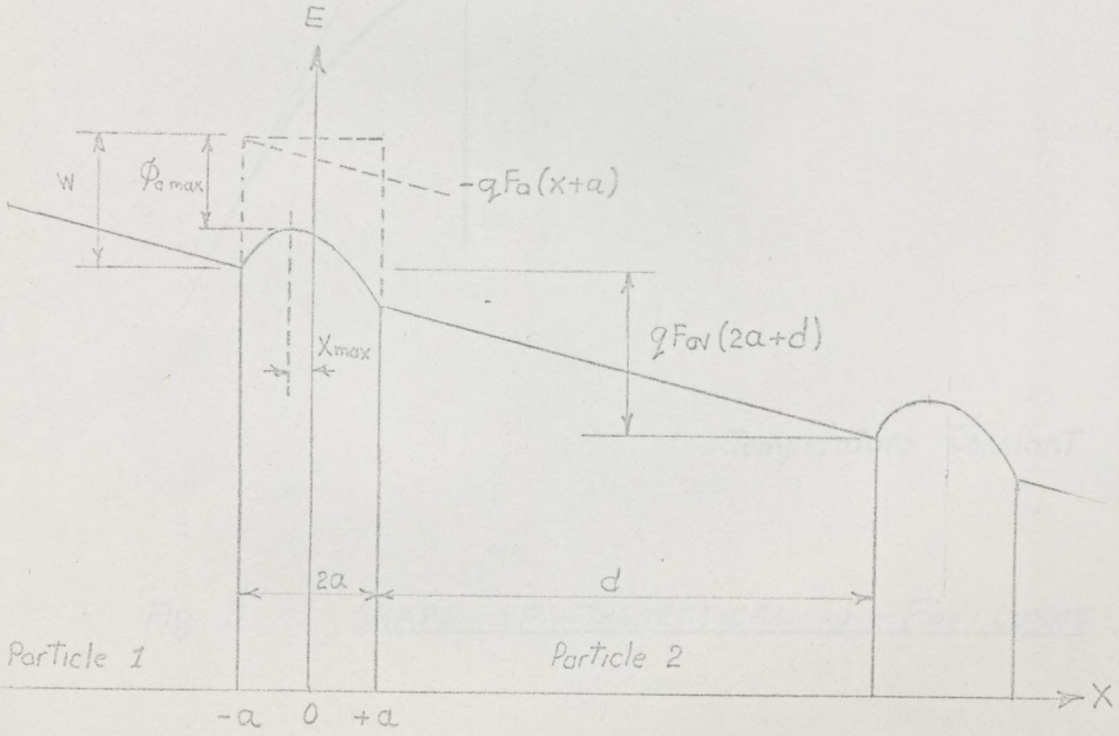

Fig 8 ENERGY LEVEL DIAGRAM WITH AN APPLIED FIELD

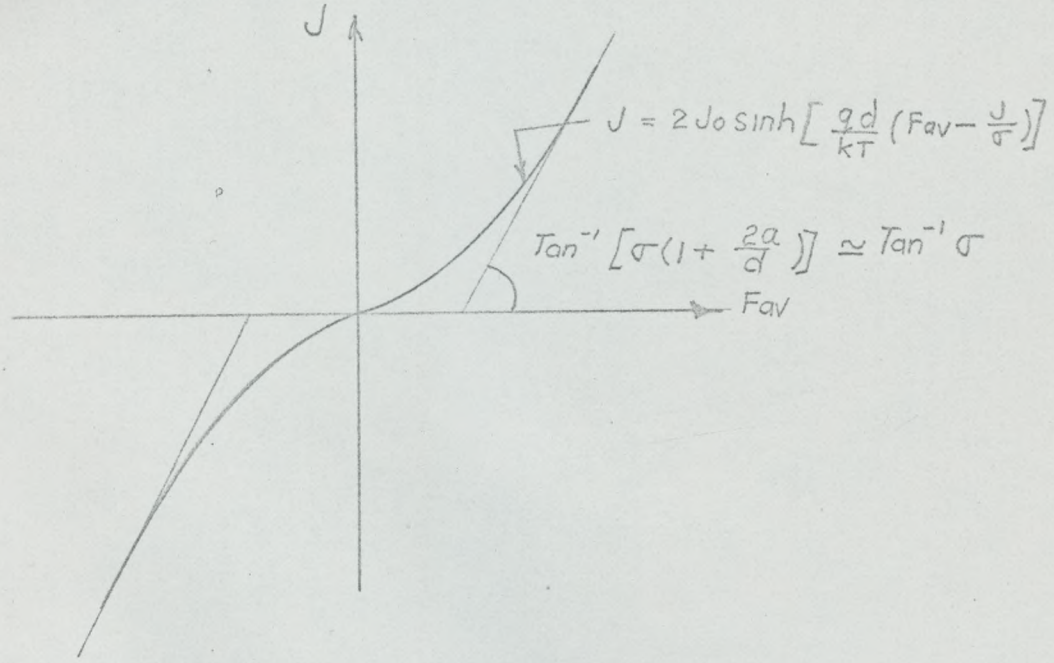

Temperature Constant

Fig. 9 SHAPE OF THEORETICAL J – Fav CURVE